

# Effects of Air Gap Spacing between a Photovoltaic Panel and Building Envelope on Electricity Generation and Heat Gains through a Building

P. Trinuruk<sup>1,\*</sup>, C. Sorapipatana<sup>1</sup> and D. Chenvidhya<sup>2</sup>

<sup>1</sup>The Joint Graduate School of Energy and Environment,  
King Mongkut's University of Technology Thonburi, Bangkok, Thailand,

<sup>2</sup>Clean Energy Systems Group (CES),  
King Mongkut's University of Technology Thonburi, Bangkok, Thailand

\*Corresponding author: cherry\_piyatida@yahoo.com

**Abstract:** The benefits of photovoltaic systems are not only for electricity generation, but also provide shading for building envelopes to reduce heat gain from solar radiation. However, a crucial problem of photovoltaic system installation on building envelopes is an increase of photovoltaic module's temperatures due to insufficient ventilation. An appropriate air spacing of the enclosure, which minimizes the heat gains through walls/roofs and maximizes photovoltaic electricity generation, has not been studied extensively and is not well documented. In this study, an adjustable testing rig model was designed and constructed. It is capable of varying the air space and the inclination angle of a photovoltaic system. The test rig was initially set up to be tilted nearly at the same degree of Bangkok's latitude

(orientated due to southward, at 15° of tilted angle) and spacing of air gap 140 mm. An actual experimental test was used to verify a simulation model. The experimental results indicate that the model can predict relatively well for the module's temperatures, but with some discrepancy for the wall surface temperatures. After that it was simulated under the same conditions with various spacings of the air gap from 10 mm to 250 mm with 10 mm increment. The results showed that the appropriate air gap can reduce the amount of heat transferred into the building by at least 1.85 kWh/m<sup>2</sup> per year. Although the increase of the air gap spacing tends to reduce the heat gain through the building, the spacing of the air gap is limited due to an increase of the unshaded area and increases in the outside temperatures of the building, which, in turn, cause the heat gains through the building to increase.

**Keywords:** photovoltaic, heat gain, air gap, building envelope, enclosure, energy balance method, simulation.

## 1. INTRODUCTION

In Thailand, about 60% of electricity in buildings is consumed by air conditioning loads because it is located in the hot humid tropics. There are a few possible solutions to reduce the electricity load demands of air conditioning systems, which are either to reduce heat gains through the building, or to prevent the building envelopes from exposure to the solar radiation by using shading devices. One of the possible methods is to mount photovoltaic panels to cover building envelopes, which is known as photovoltaic cladding. This method can

reduce amounts of the direct sunlight incident on the building envelope and, at the same time, it can also provide clean electricity generation.

Nevertheless, there is a disadvantage in mounting the photovoltaic panel on the building envelope. It will increase the photovoltaic module's temperature due to the long wave emissive radiation from the building envelope to the photovoltaic panel, if the ventilation is insufficient on the back of the photovoltaic panel. Photovoltaic performance is generally deteriorated due to the rise of the module's temperature, i.e. 0.3-0.6% per 1°C for crystalline silicon and 0.2% per 1°C for thin film silicon [1]. The performance of photovoltaic panels on the building can be improved, if there is a sufficient width of the air gap underneath the photovoltaic modules. A sufficient air gap can lead to dissipation of the heat from the photovoltaic panel, and a decrease in the module's temperatures. However, the width of the air gap between the photovoltaic module and the building envelope should not be too large otherwise it may lead to an unaesthetic appearance, damage caused by the lift-force of wind, and an increase in unshaded areas resulting in more direct solar radiation incident on the building envelope, which causes an increase in the heat gain through the building.

The influences of installed photovoltaic panels on the heat transfer through a building envelope and photovoltaic performance has been studied. The effect of an air flow induced by free convection behind the photovoltaic panels has been studied by Brinkworth et al. [2]; they found that the air flow induced by buoyancy force can reduce the module's temperature up to 20 K. Yang et al. [3] built a test rig of a photovoltaic-wall and photovoltaic-roof for validation of their

simulation model. Good design of the ventilated photovoltaic-wall structure can reduce the module's temperature up to 15°C and increase 8.0% of the power output compared with non-ventilation. The results of Brinkworth's study [2] have presented not only the effect of the module's temperature, but also the effect of shading by the photovoltaic cladding. It is noted that the peak temperature of the outer surface of the wall is reduced from 50°C to 32°C without and with PV shading, respectively, and heat gain received through a building of 105.6 kJ/m<sup>2</sup> is reduced over a day. The closing and opening of the entrance of the air gap in between the photovoltaic module and the building envelope also influences the module's temperature. Brinkworth et al. [4] found that the temperature difference between the closed and open air entrance was 26°C. This high temperature difference occurred because closing the air entrance led to poor heat transfer on the rear surface of the photovoltaic module.

In this paper, the appropriate air gap underneath photovoltaic panels on a building envelope has been investigated using a simulation method whose validity is verified by experimental results. The appropriate air gap is required in order to minimize the heat gain penetrating into the building and maximize the electricity generation from the photovoltaic panels. The present work is focused on the gap configuration in the enclosure of the non-ventilated air gap, which is the condition of the poorest photovoltaic installation on a building envelope. The inclined surface is set at 15° and the air gap is varied from 10 to 250 mm with 10 mm increments. A simulation model has been developed based on the energy balance method with the assumptions of unsteady state conditions and one-dimensional heat transfer.

## 2. METHODOLOGY

### 2.1 Experimental set up

A test rig of a photovoltaic panel on a building envelope was set up and tested in the actual outdoor climatic conditions of Thailand, at Bangkhuntain campus, King Mongkut's University of Technology Thonburi (KMUTT). Testing data were recorded automatically using Campbell datalogger "CR10X", which was programmed to read data every 10 seconds and the collected data were sampled every one minute and averaged one hour. The test rig contains an 80-W multi-crystalline silicon photovoltaic module which is mounted on lightweight blocks. The blocks were plastered by concrete mortar on both the front and the rear surface, which are a basic method of the building envelope constructed in Thailand. A room beneath the building envelope platform was constructed and enclosed with multilayer insulators and controlled at a constant temperature at 25°C, by an air conditioning unit. The periphery of the air gap, which is the space between the photovoltaic module and the building envelope, was enclosed with insulation as an enclosure space.

The constructed testing rig is supported by four steel stands, and the rig was designed in such a way that it can be adjustable in various inclination angles and air gap spaces as shown in Fig.1. A pyranometer is mounted on the same plane as the photovoltaic panels. K-type thermocouples were adhered at the middle of each surface such as the front and the rear of the photovoltaic panel, the front and the rear of the building envelopes within the enclosure air gap, and the temperature-controlled free space room.

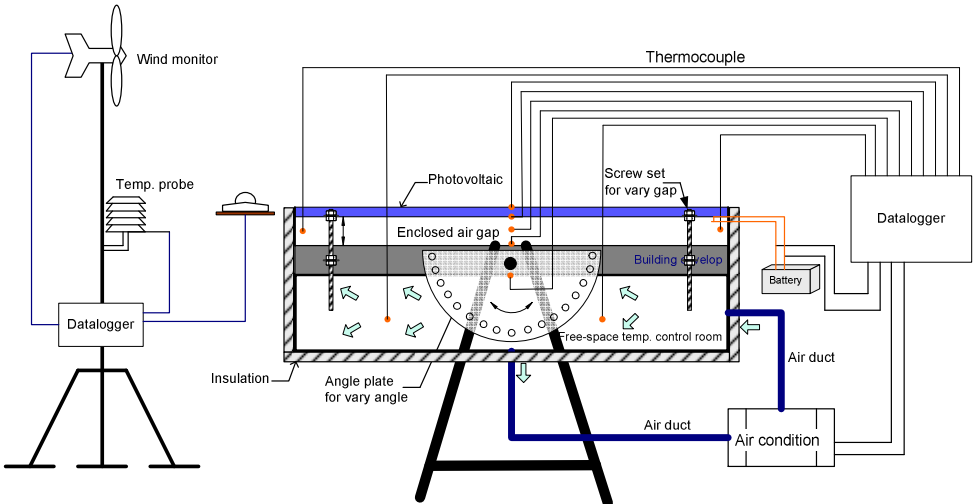


**Figure 1.** System schematic of a photovoltaic panel on building envelope.

For the measurement of climatic data, a Campbell weather station was set up to measure the wind velocity and direction, the solar irradiance, the ambient temperature, and the relative humidity, and recorded by a Campbell datalogger.

## 2.2 Testing Conditions

In the present work, the photovoltaic testing rig was set up in a condition in which a photovoltaic panel on a building envelope has the poorest ventilation, i.e. there is no ventilation beneath the photovoltaic panel at all. This condition leads to a high temperature of the photovoltaic panel and poor heat exchange to the surroundings when the sky is clear during the day time, and hence it decreases the photovoltaic performance. The air gap underneath the photovoltaic module of the test rig was enclosed around with insulation foam on the outside perimeter of all walls as shown in Fig. 2. The air gap is 140 mm high

and is tilted at an inclination of 15 degrees facing due south. Under this condition, the photovoltaic panel receives the highest solar irradiance. Measurements of the actual temperatures of each surface, the amounts of generated electricity and the weather data were recorded and used for verifying the accuracy of the simulation model.

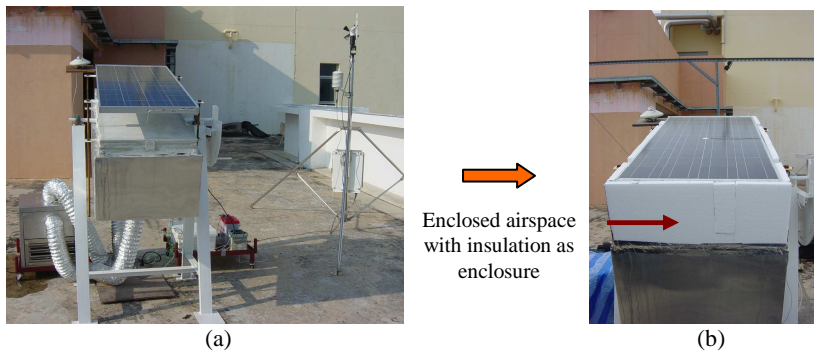


**Figure 2.** (a) Photovoltaic panel on building envelope in the field test, and (b) Setting the air gap as an enclosure.

## 2.3 Process of heat transfer on photovoltaic panel and the building

### 2.3.1 Energy balance on photovoltaic panel

The energy absorbed on a photovoltaic panel, which can all be converted into electricity, the accumulated heat on itself and the heat losses to surroundings can be written as:

$$\dot{I}_t \alpha \tau_{pv} = h_{cf} (T_{pv} - T_{amb}) + h_{rf} (T_{pv} - T_{sky}) + h_{cal} (T_{pv} - T_a) + h_{ra} (T_{pv} - T_{wo}) + \dot{I}_t \eta_{STC} (1 - 0.005(T_{pv} - 25)) + \frac{m_{pv} C_{pv} dT_{pv}}{A_{pv} dt}, \quad (1)$$

where  $\dot{I}_t$  is the solar radiation incident on the tilted surface ( $\text{W}/\text{m}^2$ ),  $\alpha$  is the absorptivity of the cell (-),  $\tau_{pv}$  is the transmissivity of the glass (-),  $h_{cf}$  and  $h_{rf}$  are respectively the heat convection coefficient and the

thermal radiation coefficient on the front surface of the photovoltaic panel ( $W/K.m^2$ ),  $h_{ca1}$  is the heat convection coefficient in the enclosed air gap between the rear surface of the photovoltaic panel and the air ( $W/K.m^2$ ),  $h_{ra}$  is the thermal radiation coefficient between the photovoltaic panel and the top surface of the top wall ( $W/K.m^2$ ),  $T_{pv}$  is the module's temperature ( $^{\circ}C$ ),  $T_{amb}$  is the ambient temperature ( $^{\circ}C$ ),  $T_{sky}$  is the sky temperature ( $^{\circ}C$ ),  $T_a$  is the air temperature in the enclosed air gap ( $^{\circ}C$ ),  $m_{pv}$  is the mass of the photovoltaic panel (kg),  $C_{pv}$  is the heat capacity of the photovoltaic panel ( $J/kg.K$ ),  $A_{pv}$  is the surface area of the photovoltaic panel ( $m^2$ ),  $\eta_{STC}$  is the photovoltaic panel's efficiency at the standard testing condition (-), and  $dt$  is the interval time (sec).

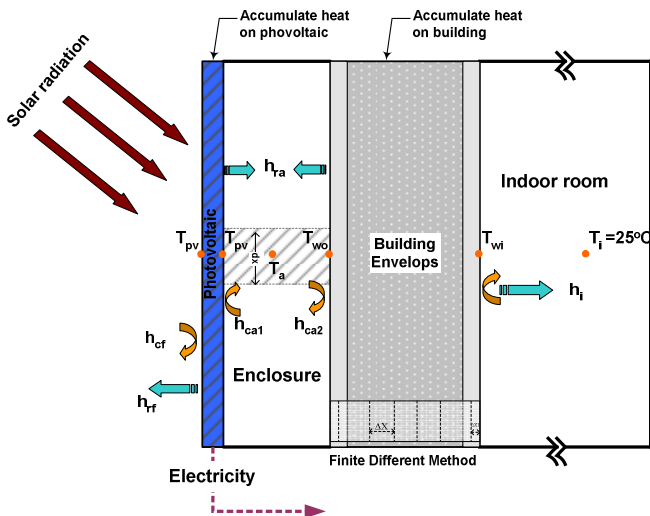


**Figure 3.** The heat transfer processes on the photovoltaic module on building envelope.

*Shortwave radiation*,  $\dot{F}_g^{\&}$ , the revised ASHRAE clear sky model, that was developed from five-year data of four-province solar radiation during years 1996-2000 by Amarananwatana et al.[5], is applied in this work to determine the solar intensity of Thailand under clear sky condition.

$$\dot{I}_g = \dot{I}_b \cos \theta_z + \dot{I}_d \quad , \quad (2)$$

$$\dot{I}_b = A \exp(-B \sec \theta_z) \quad , \quad (3)$$

$$\dot{I}_d = C \dot{I}_b \quad , \quad (4)$$

where  $\dot{F}_g^{\&}$  is the global irradiance on horizontal surface ( $\text{W}/\text{m}^2$ ),  $\dot{F}_b^{\&}$  is the direct irradiance on horizontal surface ( $\text{W}/\text{m}^2$ ),  $\dot{F}_d^{\&}$  is the diffuse irradiance on horizontal surface ( $\text{W}/\text{m}^2$ ),  $A$ ,  $B$  and  $C$  are the correction factors due to extraterritorial irradiance, atmospheric attenuation, and diffuse radiation, respectively, and  $\theta_z$  is the zenith angle (degree).

*Ambient temperature*,  $T_{amb}$ , the ASHRAE air temperature model [6] is used to calculate the outdoor air temperature for the extreme condition, which is given by

$$T_{amb} = T_{\max} - \frac{f}{100} (T_{\max} - T_{\min}) \quad , \quad (5)$$

where  $T_{\max}$  and  $T_{\min}$  are the maximum and minimum temperature from the local meteorological data ( $^{\circ}\text{C}$ ), and  $f$  is the daily range.

*Sky temperature*,  $T_{sky}$ , is based on Idso-Jackson model [7], which was an empirical formula of downward radiation, developed from experiment data based on a theoretical study of those parameters which influence on the emissivity of the atmosphere.

$$T'_{sky} = \sqrt[4]{\frac{R_o + (\sigma T'^4 - R_o)F}{\sigma}}, \tag{6}$$

when

$$R_o/\sigma T'^4 = 1 - 0.261 \text{Exp}[-7.77 \times 10^{-4} (273 - T')^2], \tag{7}$$

where  $R_o$  is the downward atmospheric radiation flux from a clear sky,  $T'$  is the absolute screen level air temperature (K),  $F$  is the correction factor from the effect of cloud [8], and  $\sigma$  is the Stefan-Boltzmann constant.

*Heat convection coefficient*, the heat convection on its surface,  $h_{cf}$ , is dominated by the effect of wind velocity,  $V_w$ , which is given by McAdams [9]

$$h_{cf} = 5.7 + 3.8V_w \quad ; \text{ for } 0 < V_w < 7 \text{ m/s}, \tag{8}$$

In an enclosed air gap, under a situation dominated by free convection, the heat transferred is calculated from the effect of the inclination angle and dimensionless numbers: the Nusselt number,  $Nu$ , the Rayleigh number,  $Ra$ , and the Prandtl number,  $Pr$ .

**Table 1.** Heat coefficient equations of free convection in the enclosure in various planes [10].

	Equation	Condition
<b>Inclined Surface</b>	$Nu = 1 + 0.446(1 - (1,708 / Ra \cdot \cos \beta))$	$1,708 \leq Ra \cdot \cos \beta < 5,900$
	$Nu = 0.229(Ra \cdot \cos \beta)^{0.252}$	$5,900 \leq Ra \cdot \cos \beta < 9.24 \times 10^4$
	$Nu = 0.157(Ra \cdot \cos \beta)^{0.285}$	$9.24 \times 10^4 \leq Ra \cdot \cos \beta < 10^6$

Therefore, the heat convection coefficient is calculated from the equation which is given by

$$h = \frac{Nu.k}{S}, \quad (9)$$

where S is the width of air gap space (m).

*Longwave radiation coefficient*, there are two longwave radiation coefficients which are involved in the calculation: the first one is  $h_{rf}$ , the longwave radiation coefficient between the photovoltaic module and the ambient, which can be expressed as

$$h_{rf} = \sigma \varepsilon_{pv} (T_{pv}'^2 + T_{sky}'^2) (T_{pv}' + T_{sky}'), \quad (10)$$

The second one is  $h_{ra}$ , the heat radiation coefficient between the rear surface of the photovoltaic module (or Tedlar) and the top wall surface of the building material that can be written as:

$$h_{ra} = \frac{\sigma (T_{pv}'^2 + T_{wo}'^2) (T_{pv}' + T_{wo}')}{(1/\varepsilon_{td}) + (1/\varepsilon_{slab}) - 1}, \quad (11)$$

where  $\varepsilon$  is the emissivity of surface material.

### 2.3.2 Energy balance of the air mass in the gap space

The air gap is assumed to be perfectly enclosed; the air flow in the gap, therefore, can be ignored. The heat balance of air in the enclosure can be calculated from the accumulated heat in the air mass in the enclosure and the absorbed (or emitted) heat transferred from the photovoltaic module and the building envelope, which is given by

$$h_{ca1} (T_{pv} - T_a) + h_{ca2} (T_{wo} - T_a) = \frac{m_a C_a}{A_{pv}} \frac{dT_a}{dt}, \quad (12)$$

where  $h_{ca2}$  is the convection coefficient of the top surface of the wall with the air in the enclosure (W/K.m<sup>2</sup>), and  $m_a$ ,  $C_a$ , and  $T_a$  are the mass,

the heat capacity and the temperature of the air in the enclosure respectively.

### 2.3.3 Energy balance on the top surface of the top wall (or roof)

The heat balance on the top of the top wall (roof) surface can be calculated from the long wave radiation exchanges between the photovoltaic panel's rear surface and the top wall's surface, the heat convection of air at the top wall's surface within the enclosed air gap, and the heat penetration (released) by conduction into (from) the surface of the top wall (roof) to the first inner layer of building materials at temperature node of  $T_{1,j}$ ;

$$h_{ca2}(T_a - T_{wo}) + h_{ra}(T_{pv} - T_{wo}) = (T_{wo} - T_{1,j}) / R_{1a}, \quad (13)$$

where  $R_{1a}$  is the thermal resistance of the 1<sup>st</sup> wall layer (K.m<sup>2</sup>/W),  $T_{i,j}$  is the temperature at a given inner layer  $i^{\text{th}}$  and at a point  $j$  (°C).

*Heat conduction coefficient of the building material*, can be calculated from the conductance of material, with respect to its thickness. The transient heat transfer is applied and a wall layer can be assumed to be at a single uniform temperature, provided that its Biot number,  $Bi$ , is less than 0.1:

$$Bi = \frac{hL}{k}, \quad (14)$$

where  $h$  is the heat convection coefficient (W/K.m<sup>2</sup>),  $L$  is the characteristic length of the object (m), and  $k$  is the thermal conductivity of the material (W/K.m).

The heat conduction resistance of the material,  $R$ , is

$$R = \frac{L}{k}. \quad (15)$$

### 2.3.4 Energy balance in the building material

Normally, the heat transfer across the building material (wall/roof) can be simplified by one-dimensional analysis. The wall comprises of several thin sections of homogeneous material, and each of them can be represented by a single temperature for the entire interior of that section. In this study, the finite difference method is applied in the simulation model to study the heat transfer in the building material. The energy balance for an interior point can be computed from the heat balance of the accumulated heat in the layer and the heat conduction as given below:

$$\frac{\Delta x \rho C_p}{dt} (T_{i,j} - T_{i,j-1}) = \frac{T_{i-1,j} - T_{i,j}}{R_{i-1,b} + R_{i,a}} - \frac{T_{i,j} - T_{i+1,j}}{R_{i,b} + R_{i+1,a}}, \quad (16)$$

where  $\Delta x$  is the thickness of wall layer (m).

### 2.3.5 Energy balance on an inner surface of the wall

The heat balance on an inner surface of the wall is dominated by the heat conduction and the heat transfer coefficient of the combination between the convection and the radiation in the indoor room,  $h_i$ , which is given by

$$h_i (T_{wi} - T_i) = \frac{T_{n,j} - T_{wi}}{R_{n,b}}, \quad (17)$$

where  $T_i$  is the room temperature, which is fixed at 25°C,  $T_{wi}$  is the surface temperature of the inner wall (°C).

### 2.3.6 The heat gain through building

According to the heat conduction, the calculation of this simulation is examined by using the finite difference method. The heat gain through the building can be computed from the heat transfer between the surface temperature of the inner wall and the air temperature inside the room.

$$q'' = h_i(T_{wi} - T_i), \quad (18)$$

where  $q''$  is the total heat flux into the building ( $\text{W}/\text{m}^2$ ).

### 2.4 The simulation method

The simulation model was programmed by using MATLAB software, based on the above equations as shown in Fig.4. The program can determine the annual heat gain through the building and the annual electricity energy outputs from the photovoltaic panel mounting on the building envelope under the clear sky condition of Thailand, which is considered to be the maximum possible electricity outputs available, while minimizing the heat load transferred to the building envelope. The model is based on the following assumptions: (i) the heat transfer is one-dimensional, (ii) the thermal-physical properties of photovoltaic elements and building materials are independent of temperature within the test conditions, (iii) the temperatures are uniformly distributed within the materials, (iv) the temperature difference between the front and the rear surface of the module is neglected and (v) the effect of heat capacity from the aluminum frame of the photovoltaic panel is ignored. The physical properties of photovoltaic components and the building materials are given in Table 2.

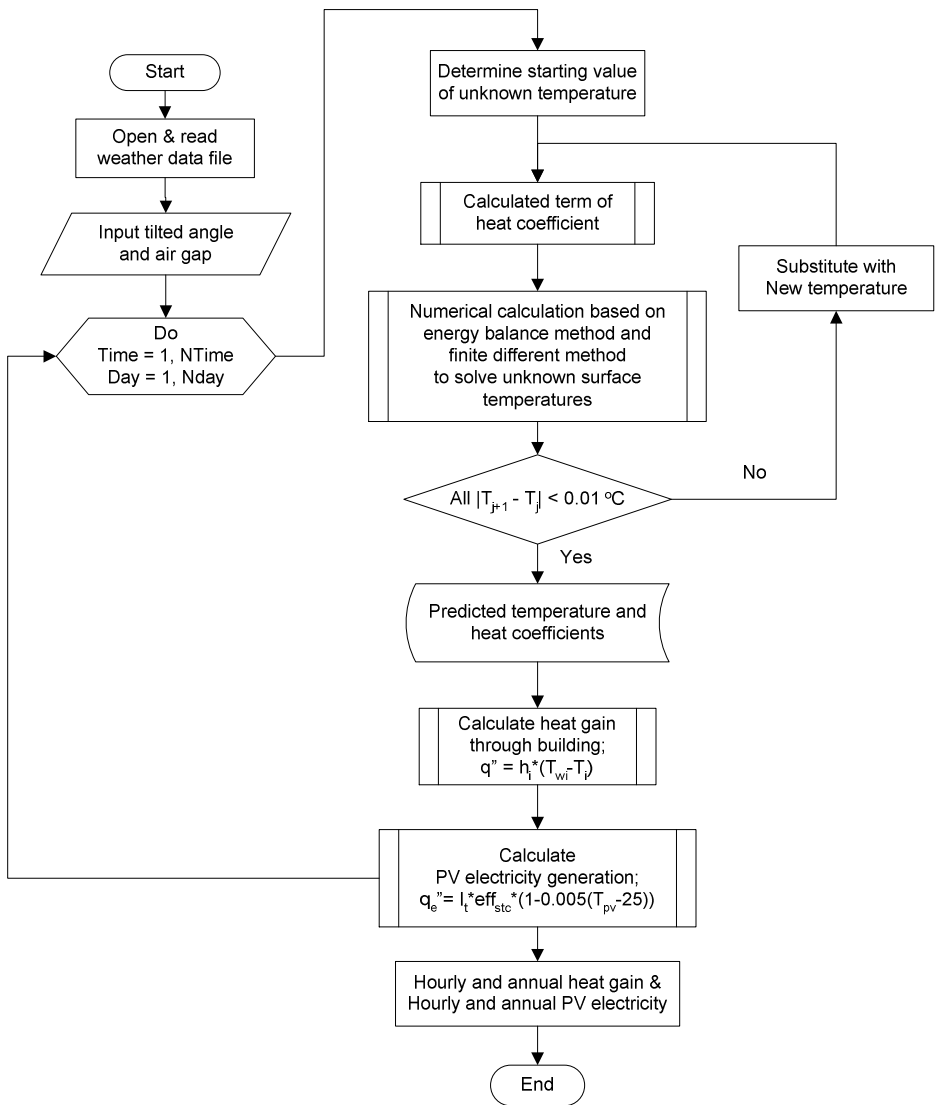


**Figure 4.** Flow diagram of simulation program.

**Table 2.** Physical properties of photovoltaic components and building materials [11-14].

	Unit	Glass	Photovoltaic cell	Tedlar	Lightweight block	Concrete plastering
Thickness	m	0.006	0.00038	0.00017	0.075	0.01
Density	kg/m <sup>3</sup>	2,500	2,330	1,475	1,400	700
Specific heat	J/kg.K	840	712	1,130	962	1,000
Thermal conductivity	W/m.K	1.04	148	0.14	0.42	0.2
Absorptivity, $\alpha$	-	0.8	-	-	-	0.4
Transmittivity, $\tau$	-	-	-	-	-	-
Emissivity, $\varepsilon$	-	0.94	-	0.893	0.93	0.93

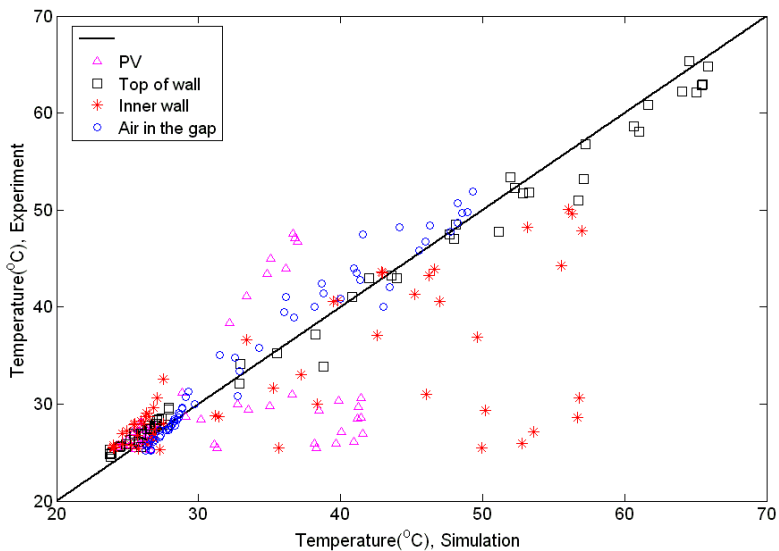
### 3. RESULTS OF STUDY

#### 3.1 Accuracy of simulation model and verification

Prior to using the simulation model for evaluating the amount of annual heat flux passing into a building and the annual electricity generating under the extreme condition of Thailand, the model accuracy should be verified with experimental data. The model performance is assessed by using experimental data under the testing conditions of 15° tilted angle, facing due south and 140 mm air spacing, and statistical analyses: the root mean square error (RMSE) and the mean bias error (MBE). RMSE is calculated to assess the magnitude of the accuracy of the predicted data, whereas MBE is used to identify the systematic error of the predicted data: whether it is an overestimation or an underestimation of the actual values. The comparison of RMSE, MBE, % Error of RMSE and % Error of MBE of the predictions with the corresponding mean values, between the module's temperature and the top of the wall temperature is given in Table 3 and shown in Fig. 5.

**Table 3.** Verifying the model accuracy with the mean of the experimental data, RMSE, MBE, % Error of RMSE and MBE.

	Module's temperature	The top of the wall surface temperature	The inner of the wall surface temperature	The air temperature in the air gap
<b>Number of Observations</b>	56	56	56	56
<b>Mean (°C)</b>	38.937	35.036	27.062	35.322
<b>RMSE (°C)</b>	1.843	4.816	6.780	2.141
<b>MBE (°C)</b>	-0.091	0.744	0.854	-1.000
<b>% Error of RMSE</b>	5.324	15.309	25.542	6.563
<b>% Error of MBE</b>	-0.401	2.151	10.340	-2.962

**Figure 5.** The correlation between the simulation results and experimental results in the temperature predictions.

The average value of RMSE of the module's temperature is 1.843°C, the RMSE of the surface temperature of the top wall is

4.816°C, the RMSE of the surface temperature of the inner wall is 6.708°C, and the RMSE of the air temperature in the gap is 2.141°C. This indicates that the simulation model gives a better accuracy in the prediction of the module's temperature than the air temperature in the enclosed air gap, the surface temperature of the top wall, and the surface temperature of the inner wall, respectively. The magnitude of MBE is -0.091°C for the module's temperature, 0.744°C for the surface temperature of the top wall, 0.854°C for the surface temperature of the inner wall and -1.000°C for the surface temperature of the inner wall, respectively. The simulation model, therefore, has a slight systematic error in underestimating the module's temperature, whereas, it overestimates the surface temperature of the top wall.

### **3.2 The effect of spacing of the air gap**

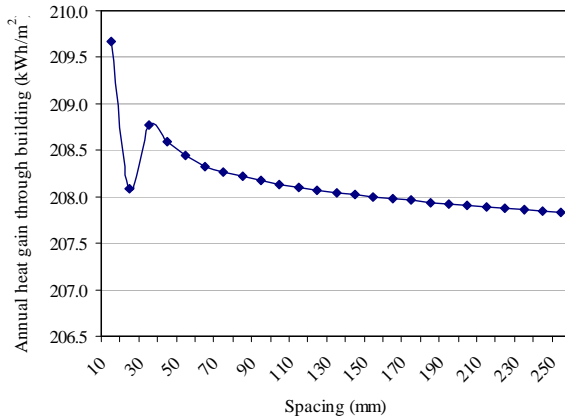
The model is simulated continuously over an entire year under the maximum solar radiation of the clear sky condition of Thailand to evaluate the annual amounts of heat transferred through the building, and the annual amounts of photovoltaic electrical energy generation from the photovoltaic panel on the building envelope. The inclined surface of the photovoltaic panel was tilted at 15°, the air gap was varied from 10 mm to 250 mm, with 10 mm increments, and the wind speed was fixed at 1 m/s to investigate the effect of the air gap's spacing.

The correlation between the annual amount of heat gains through the building per unit area and the air space is shown in Fig. 6. It indicates that the annual amount of the heat gain penetrating

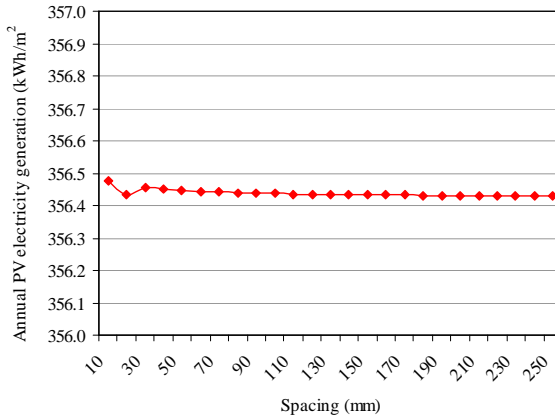
through the top of the building envelope is not linearly proportional to the gap spacing. At a very small air gap, the annual amount of the heat gains through the building is as high as 209.7 kWh/m<sup>2</sup>, and the heat flux decreases sharply, as the air gap increases until it is at a critical gap of 20 mm, then the annual heat flux increases sharply again, as soon as the air gap increases to another critical gap spacing at 30 mm. At this spacing, the heat flux increases to the second peak of 208.7 kWh/m<sup>2</sup>, which is slightly less than the first peak. At higher air gap spacings the heat flux through the building will gradually decrease with the increasing of the air gap.

The sharp decrease in the annual amount of heat flux at a very small gap indicates that the heat transfer process is dominated by heat conduction. The effect of the heat conduction then decreases, because of increasing of the air gap's height. However, when the height of the air gap is large enough, it starts to initiate heat convection in laminar flow, and subsequently convection becomes dominant leading to the increase in the overall heat transfer coefficient. Thereafter, as the spacing increases the value of the heat convection coefficient gradually decreases because the effect of the spacing gap is dominant over the Nusselt number.

In contrast, the annual amount of the electrical energy generated by the photovoltaic panel is considerably less variable with increasing of the air gap compared with the annual amounts of the heat flux penetrated through the building envelope. Thus, an increase in the air gap provides a better generation of the annual amount of photovoltaic electrical energy generating, which is about 0.05 kWh/m<sup>2</sup>.



(a) Annual heat gains through building



(b) Annual electricity generation from photovoltaic

**Figure 6.** The simulation results of the annual amount of heat flux penetrated into a building envelope and the annual amount of the electricity generation from the photovoltaic panel on the same building envelope, at 15° tilted angle, under a clear sky condition of Thailand, at 1 m/s of wind speed.

## 4. CONCLUSIONS

This study showed that the simulation method developed gives the most accurate results on the prediction on the module's temperature among all predicted parameters such as the temperatures of the air gap, the temperatures of the top and internal surface of the wall.

The simulation results for the totally enclosed air gap underneath the photovoltaic panel, which is equivalent to the worst condition, without any ventilation beneath the photovoltaic panel, indicate that the appropriate air gap can reduce the heat flux through the building, which in turn could reduce the load of an air conditioning system of a building, at least  $1.85 \text{ kWh/m}^2$  in a year. However, the air gap does not give any significant effects in increasing amounts of electricity energy generated from a photovoltaic panel. Although the photovoltaic panel can reduce only a relatively small amount of the heat gain through the building, its good advantage is that it can provide some of clean electricity energy from the photovoltaic panel, which is about  $356 \text{ kWh/m}^2$  per year.

For the case of Thailand, where the inclined surface of the photovoltaic panel should be tilted at about  $15^\circ$  and wind speed is generally low, a spacing of the appropriate air gap should be more than 40 mm to reduce heat transfer from the back of the photovoltaic panel to the building envelope. In order to minimize the heat gain, a larger air gap is preferred. Although larger air gaps are preferable to give lower heat gains through the building, it should be kept in mind that if the air gap is too large, it could give a negative effect on

increasing of heat gain, since it will reduce a projected shaded area due to the slant of solar irradiance incident on the building envelope.

## 5. ACKNOWLEDGEMENTS

P.T. thanks to Prof. Dr. R.B.H Exell, and Dr. Pattana Rukkwamsuk for their helpful suggestions and many comments.

## 6. REFERENCES

- [1] The German Solar Energy Society and Ecofys (2005) *Planning and Installing Photovoltaic System: A Guide for Installers, Architects, and Engineers*, James & James (Science Publishers) Ltd., England.
- [2] Brinkworth, B.J., Cross, B.M., Marshall, R.H., and Yang, H.X. (1997) Thermal Regulation of Photovoltaic Cladding, *Solar Energy*, **61**(3), pp.169-178.
- [3] Yang, H.X., Marshall, R.H. and Brinkworth, B.J. (1996) Validated Simulation for Thermal Regulation of Photovoltaic Wall Structures, *25<sup>th</sup> PVSC, May 13-17, Washington, D.C.*, pp. 1453-1456.
- [4] Moshfegh, B. and Sandberg, M. (1996) Investigation of Fluid Flow and Heat Transfer in A Vertical Channel Heated From One Side By PV Elements: Part I Numerical Study, *WREC*, pp. 248-253.
- [5] Amarananwatana, P. and Sorapipatana, C. (2005) *An Assessment of The ASHRAE Clear Sky Model for Irradiance Prediction in Thailand*, The Joint Graduated School of Energy and Environment, KMUTT, Thailand.
- [6] ASHRAE (1993) *1993 ASHRAE Handbook-Fundamental*, Atlanta, American Society of Heating, Refrigerating and Air Conditioning Engineering, Inc.
- [7] Idso, S.B. and Jackson, R.D. (1969) Thermal Radiation from the Atmosphere. *J. Geophys. Res.*, **74**, pp. 5397-5403.

- [8] Exell, R.H.B. (1978) Atmospheric Radiation in a Tropical Climate, *AIT Research Report*, **71**.
- [9] Duffie, J.A. and Beckman, W.A. (1991) *Solar Engineering of Thermal Processes*, 2<sup>nd</sup> ed., John Wiley & Sons, Inc., USA.
- [10] Nijaguna, B.T. (2005) *Thermal Science Data Book*, Tata McGraw-Hill, India.
- [11] Davis, M.W., Dougherty, B.P., and Fanney, A.H. (2003) Measured Versus Predicted Performance of Building Integrated Photovoltaic, *Journal of Solar Energy Engineering by ASME*, **125**, February, pp. 21-27.
- [12] Jones, A.D. and Underwood, C.P. (2001) A Thermal Model for Photovoltaic Systems, *Solar Energy*, **70**(4), pp. 349-359.
- [13] Davis, M.W., Dougherty, B.P., and Fanney, A.H. (2001) Prediction of Building Integrated Photovoltaic Cell temperatures, *Trans. ASME J. Heat Transfer*, **123**, August, pp. 200-210.
- [14] Kreider, J.F. (2001) *Handbook of Heating Ventilation and Air Conditioning*, CRC Press LLC, USA, pp. 8-19.